

See discussions, stats, and author profiles for this publication at: <https://www.researchgate.net/publication/6538857>

# Microbicides for HIV/AIDS. 2. Electrophoretic fingerprinting of CD4<sup>+</sup>T-cell model systems

ARTICLE *in* LANGMUIR · MARCH 2007

Impact Factor: 4.46 · DOI: 10.1021/la063043n · Source: PubMed

CITATIONS

3

READS

22

9 AUTHORS, INCLUDING:



**David Fairhurst**

Particle Sciences Inc.

30 PUBLICATIONS 592 CITATIONS

SEE PROFILE



**Anastasia Morfesis**

Carnegie Mellon University

14 PUBLICATIONS 219 CITATIONS

SEE PROFILE



**Mark Mitchnick**

Particle Sciences Inc.

23 PUBLICATIONS 741 CITATIONS

SEE PROFILE



**Robin Shattock**

Imperial College London

5 PUBLICATIONS 15 CITATIONS

SEE PROFILE

## Microbicides for HIV/AIDS. 2. Electrophoretic Fingerprinting of CD4+ T-Cell Model Systems

D. Fairhurst,<sup>\*,†</sup> R. L. Rowell,<sup>\*,‡</sup> I. M. Monahan,<sup>§</sup> S. Key,<sup>§</sup> D. Stieh,<sup>§</sup> F. McNeil-Watson,<sup>||</sup> A. Morfesis,<sup>||</sup> M. Mitchnick,<sup>⊥</sup> and R. A. Shattock<sup>§</sup>

*International Partnership for Microbicides, Silver Spring, Maryland 20910, Department of Chemistry, University of Massachusetts, Amherst, Massachusetts 01003, St. George's Hospital, University of London, London SW17 0RE, United Kingdom, Malvern Instruments Ltd., Malvern WR14 1XZ, United Kingdom, and Particle Sciences Inc., Bethlehem, Pennsylvania 18017*

*Received October 16, 2006. In Final Form: December 11, 2006*

New measurements of the dependence of the surface charge on the pH and electrolyte concentration for three living human white blood cell lines that are the principal targets of the HIV-1 virus are reported. Comparison of the electrophoretic fingerprint (EF) pattern, especially the line of zero mobility, with that of reference colloids establishes the separate individual identities and shows that all three exhibit a zwitterionic surface. With the EF results as a guide, preliminary biological infectivity measurements showed that small polyvalent cations modulate the negative charge on the T-cell surface in a way that strongly affects the infection kinetics. H9 cells were exposed to an infectious virus (X4), and the data showed that HIV interaction with target cells is enhanced by physiological fluids. The nondestructive methodology described is generally applicable to characterization of the surface charge and determination of the colloidal stability of any aqueous charged colloidal system without reference to any model of the double layer.

### Introduction

The growing development of the multidisciplinary, and frequently international, study of the biomolecular interface has largely centered on the science of planar surfaces,<sup>1</sup> but new insights are also emerging from bioparticles. Polymeric encapsulation of single living cells of baker's yeast has demonstrated that encapsulated cells can preserve metabolic activity and remain able to divide.<sup>2</sup> Methods for preparing live cellular arrays for fundamental studies and for pharmaceutical drug development have been reviewed, and a new electrooptical method has been used to array mammalian cells by electrophoresis by taking advantage of the intrinsic negative surface charge of the cells.<sup>3</sup> Closer to our work has been the separation of human T- and B-lymphocytes using microfluidic chambers, which is important in analyzing the progression of HIV (human immune deficiency) infection and transplant rejection.<sup>4</sup> Our work on the characterization of the surface charge by nondestructive electrophoretic fingerprinting (EF) of living human white blood cells follows with a comparison of the identification and surface-charge properties of three living white blood cell lines that are the principal targets of the HIV-1 virus.

AIDS (acquired immune deficiency syndrome) was first recognized as a new, and distinct, clinical entity in 1981.<sup>5</sup> Since

then, AIDS has claimed the lives of more than 25 million people worldwide, making it one of the largest epidemics in history. In 2005 there were 40.3 million people living with HIV-1 infection.<sup>6</sup> The mainstay of modern disease prevention is the vaccine. Unfortunately, developing a preventative HIV-1 vaccine that decisively reduces the rate of spreading of the AIDS pandemic is likely to take a decade or more.<sup>7</sup> Since the majority of new infections are transmitted through heterosexual contact,<sup>8,9</sup> there is an urgent need to develop alternative measures and technologies to prevent the sexual transmission of HIV. One concept under evaluation is that of a topical microbicide—a vaginally or rectally applied compound designed to inactivate incoming HIV-1 or to prevent the virus from entering or replicating in the cells that it infects at or near its site of deposition.<sup>10</sup> With the expansion of the epidemic and recognized difficulties in vaccine development there has been an increase in available resources,<sup>11</sup> and several strategies for microbicide development are now being actively pursued.<sup>12</sup> The most developed approaches fall into three broad categories: membrane-disruptive agents, charge-dependent inhibition of viral attachment/fusion, and the use of antiretroviral (ARV) drugs. The ARV drugs being considered as microbicides are the same, or similar to, drugs being used as therapeutics, and they include highly potent nucleoside and nonnucleoside inhibitors of reverse transcriptase. Membrane-disruptive agents work by destroying the outer envelope layer of the virus, but show little selectivity between viral and cellular membranes. In contrast, charge-dependent viral inhibition is an appealing strategy in that the virus is “stopped” in the vaginal lumen prior to entry into the host's cells. A variety of polyanions have been developed for this application,<sup>13–15</sup> and they have the advantages of being cheap to produce and highly biocompatible.

<sup>†</sup> International Partnership for Microbicides.

<sup>‡</sup> University of Massachusetts.

<sup>§</sup> University of London.

<sup>||</sup> Malvern Instruments Ltd.

<sup>⊥</sup> Particle Sciences Inc.

(1) See the special issue on “The Biomolecular Interface”: *Langmuir* **2003**, *19* (5) (March 4).

(2) Diaspro, A.; Silvano, D.; Krol, S.; Cavalleri, O.; Gliozzi, A. *Langmuir* **2002**, *18*, 5047.

(3) Ozkan, M.; Pisanic, T.; Scheel, J.; Barlow, C.; Esener, S.; Bhatia, S. N. *Langmuir* **2003**, *19*, 1532.

(4) Murthy, S. K.; Sin, A.; Tompkins, R. G.; Toner, M. *Langmuir* **2004**, *20*, 11649.

(5) Essex, M. E. In *AIDS: Biology, Diagnosis, Treatment and Prevention*, 4th ed.; DeVita, V. T., Hellman, S., Rosenberg, S. A., Eds.; Lippincott-Raven: New York, 1997; Chapter 1.

(6) UNAIDS/WHO. *AIDS Epidemic update 2005*; Geneva, 2005.

(7) Moore, J. P. *N. Engl. J. Med.* **2005**, Jan, 298.

(8) UNAIDS/WHO. *AIDS Epidemic update 2004*; Geneva, 2004.

(9) Evans, A.; Lee, R.; Mammem-Tobin, A.; Piyadigamage, A.; Shann, S.; Waugh, M. *SKINmed* **2004**, *3* (3), 149.

(10) Moore, J. P. *N. Engl. J. Med.* **2005**, *352* (3), 298.

(11) Shattock, R. A.; Moore, J. P. *Nat. Rev. Microbiol.* **2003**, *1*, 25.

(12) Davis, C. W.; Doms, R. W. *J. Exp. Med.* **2004**, *199* (8), 1037.

(13) D'Cruz, O. J.; Uckun, F. M. *Curr. Pharm. Des.* **2004**, *10* (3), 315.

(14) Turpin, J. A. *Expert Opin. Invest. Drugs* **2002**, *11* (Aug), 1077.

Polyanion microbicides are based on the premise that they are able to bind to a sterically restricted surface on the viral envelope glycoprotein that has a positive charge.<sup>16,17</sup> The polyanion–virus complex is then unable to attach to the target cell. If virus–cell interaction is thus inhibited, then HIV-1 is prevented from entering cells and it becomes, effectively, an inert particle. Since the interaction is “charge related”, one new paradigm for the selection or design of antimicrobial compounds or compositions is to assess their ability to affect the surface chemical properties of the target cell or virus.

HIV has been extensively studied in terms of its genetic content, biological activity, and structure and reactivity of its surface constituents. The amino acid sequence and tertiary structure of gp120, for instance, is well-known and is the basis for much of today's HIV vaccine and therapeutic drug development efforts. However, there have been relatively few studies of HIV as a particle with bulk surface characteristics dictated by specific surface moieties. Of equal importance to the surface characteristics of the virion are the surface characteristics of HIV's target cells, the cells that HIV initially infects. Whatever properties exist on HIV, receptive conditions must also exist on the target cells to enable physical contact—a prerequisite to infection. CD4+ T-cells are the primary target cells for HIV.

An ambitious and long-term program of study has been initiated by the International Partnership for Microbicides at St. George's Hospital, University of London, to characterize the  $\zeta$ -potential (ZP) of HIV-1 virus over a range of conditions relevant for infection, in particular encompassing those typical of the vaginal environment pre- and postintercourse. The aim of our work is to obtain direct experimental evidence of the properties of the AIDS virion in situ before, during, and after interaction with microbicides. The HIV-1 virus is extremely difficult to isolate and purify sufficiently for  $\zeta$ -potential measurements. Accordingly, the initial focus of the project has been the characterization of target cells. Preliminary results, using the technique of EF to determine the electrochemical behavior of the H9 cell line, have previously been reported.<sup>18</sup> In that paper, the EF technique was, for the first time, applied to the study of a living moiety. The results are briefly summarized below in comparison with the present work.

In the present paper, we extend the study to two further human CD4+ T-cell lines used for in vitro culture of HIV-1, viz., C8166 and Molt4, and we report the results of an in-depth, comprehensive comparison with H9, together with some preliminary biological activity measurements using H9 cells based on the results of the cell surface chemistry as determined from the EF. As in the previous study, we have attempted to keep the concentration of the colloid (the human CD4+ T-cells) constant and held as close as possible to that of the growth medium from which the experimental aliquot was withdrawn.

## Experimental Section

**Samples.** Molt4, H9, and C8166 cells are human T-cells that are particularly permissive for HIV-1 replication. Most laboratory T-cell lines express only CXCR4 receptors and are, therefore, only susceptible to X4 strains of HIV-1. This leads to these strains of HIV-1 being called T-tropic, syncytial-inducing viruses. H9, C8166,

and Molt4 cells are all capable of supporting both the infection and replication of these strains of HIV.

**H9 Cells.** These are a human cutaneous T-cell lymphoma derived from the HUT78 cell line.<sup>19</sup> They are widely used for the cultivation of HIV-1 and grow as single cells and small aggregates in suspension culture.

**C8166 Cells.** These are human T-lymphoblastoid cells derived from an adult T-cell leukemia lymphoma patient.<sup>20</sup> This cell line in particular (when infected with X4 HIV) produces large visible syncytia with a ballooning effect that results in cell death within 4–6 days of infection. They grow in large cell aggregates in suspension culture.

**Molt4 Cells.** These are a human acute lymphoblastic leukemia T-cell line.<sup>21</sup> They grow as single cells in suspension.

**Preparation of the Samples.** Cells were maintained in RPMI growth medium supplemented with 10% heat-inactivated fetal calf serum, 2 mM glutamine, 100 iu/mL penicillin, and 100  $\mu$ g/mL streptomycin at 37 °C in a humidified 5% CO<sub>2</sub> incubator. The cells were routinely maintained every 3–4 days in 75 cm<sup>2</sup> filter cap tissue culture flasks by removing 4 mL of cells and adding them to 16 mL of fresh growth medium.

Prior to electrophoretic analysis, 10 mL aliquots of the cells were spun at 1000 rpm for 5 min, and the pellets resuspended in 10 mL volumes of the appropriate NaCl concentrations under examination (1, 5, 10, 50, 100, 154, and 200 mM). The samples were also examined in distilled water. The range of ionic strengths was extended below that of usual physiological conditions to be able to more completely develop the EF. The range of pH values was chosen to cover that known for fluids found in the lower female reproductive tract, including vaginal fluid and semen.<sup>23,24</sup>

**Cell Titrations Using Lanthanum Chloride.** Aliquots of 10 mL of H9, C8166, and Molt 4 cells were spun at 1000 rpm for 5 min and then resuspended in 0.154 M NaCl that contained increasing amounts of LaCl<sub>3</sub> (10–400  $\mu$ M). The  $\zeta$ -potential of the cells was measured after incubation for 1 h at 37 °C.

**Infection of Enzyme- and Polycation-Treated H9 Cells with HIV-1<sub>RF</sub>.** A 5 mL sample of H9 cells was incubated at 37 °C for 1 h with the following final concentrations of enzymes: 10 units/mL heparinase, 250  $\mu$ g/mL collagenase, and 250  $\mu$ g/mL hyaluronidase. After this time, the cells were spun at 1000 rpm for 5 min, washed twice in PBS (phosphate-buffered saline), spun at 1000 rpm for 5 min, and resuspended in 5 mL of fresh complete RPMI. In addition to this, 5 mL of H9 cells was treated with 200 and 450  $\mu$ M LaCl<sub>3</sub> to give the cells a neutral and positive charge, respectively.

A 100  $\mu$ L sample of each of the treated H9 cell preparations was plated in a 96-well plate at  $2 \times 10^5$  cells/well. A 100  $\mu$ L portion of HIV-1<sub>RF</sub> (TCID<sub>50</sub> 10<sup>4</sup> mL<sup>-1</sup>) was added to the cells, and they were incubated for 2 h at 37 °C in 5% CO<sub>2</sub>. The cells were then washed four times in PBS at 1000 rpm for 5 min and finally resuspended in 200  $\mu$ L of RPMI. Each cell preparation was performed in triplicate, and an uninfected cell control in RPMI growth medium was also included. The supernatant was removed 7 days postinfection and assessed for HIV-1 reverse transcriptase (RT) activity, which is an indicator of viral replication.<sup>25</sup>

**Effect of Physiological Conditions on HIV-1 Binding to H9 Cells.** PM-1 cells were used. This T-cell line is a clonal derivative of the HUT78 T-cell line. It is uniquely susceptible to a wide range of HIV-1 isolates and is capable of establishing persistent infection,

(15) Neurath, A. R.; Strick, N.; Li, Y. Y.; Debnath, A. K. *BMC Infect. Dis.* **2001**, *1*, 17.

(16) Shaunak, S.; Thornton, M.; Teo, I.; Chandler, B.; Jones, M.; Steel, S. *J. Drug Targeting* **2003**, *11*, 443.

(17) Moulard, M.; Lortat-Jacob, H.; Mondor, I.; Roca, G.; Wyatt, R.; Sodroski, J.; Zhao, L.; Olson, W.; Kwong, P. D.; Sattentau, Q. *J. Virol.* **2000**, *74* (Feb), 1948.

(18) Rowell, R. L.; Fairhurst, D.; Key, S.; Morfesis, A.; Monahan, I. M.; Mitchnick, M. Shattock, R. S. *Langmuir* **2005**, *21*, 10165.

(19) Popovic, M.; Sarngadharan, M. G.; Read, E.; Gallo, R. C. *Science* **1984**, *224*, 497.

(20) Salahuddin, S. Z.; Markham, P. D.; Wong-Staal, F.; Franchini, G.; Kalyanaraman, V. S.; Gallo, R. C. *Virology* **1983**, *129*, 51.

(21) Kikukawa, R.; Koyanagi, Y.; Harada, S.; Kobayashi, N.; Hatanaka, M.; Yamamoto, N. *J. Virol.* **1986**, *1159*.

(22) Portions of the Preparation of the Samples and Instrumentation sections are from the thesis of Suzie Key, B.Sc. (Biomedical Sciences), St. George's Hospital Medical School, London, 2004.

(23) Katz, D. F.; Anderson, M. H.; Owen, D. H.; Plenys, A. M.; Walmer, D. K. In *Vaginal Microbicide Formulations Workshop*; Rencher, W. F., Ed.; Lippincott-Raven Publishers: Philadelphia, 1998.

(24) Katz, D. F.; Owen, D. H. *Contraception* **1999**, *59*, 91.

(25) Potts, B. J. In *Techniques in HIV Research*; Aldovini, A., Walker, B. D., Eds.; Stockton: New York, 1990.

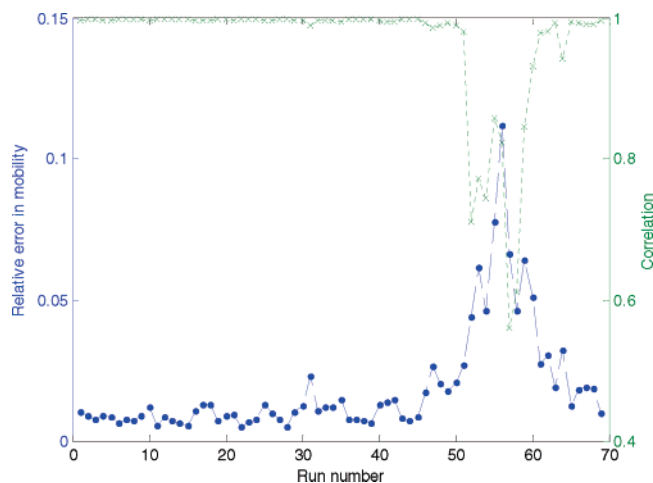


**Figure 1.** Mobility fit error (dots) and linear correlation (times signs) against the run number.

with sustained levels of viral replication over prolonged periods.<sup>26</sup> The cells were initially resuspended in physiological solutions used to mimic those encountered in various types of bodily fluids: seminal fluid (0.09 M NaCl, pH 7.7), cervical mucus (0.154 M NaCl, pH 7.0), and vaginal fluid (0.154 M NaCl, pH 5). The treated cells were plated in a 96-well plate at  $2 \times 10^5$  cells/well. A 100  $\mu\text{L}$  aliquot of HIV-1<sub>RF</sub> (TCID<sub>50</sub>  $10^3 \text{ mL}^{-1}$ ) was added to the cells, and they were incubated for 2 h at 37 °C in 5% CO<sub>2</sub>. The cells were then washed four times in PBS at 1000 rpm for 5 min and finally resuspended in 100  $\mu\text{L}$  of PBS. The cells were lysed by the addition of Triton-X to a final concentration of 1%, and HIV-1 binding was assessed by p24 ELISA (SAIC-Frederick Inc., Frederick, MD), according to the manufacturer's instructions. Each test was performed in triplicate, and the control was uninfected PM-1 cells in RPMI growth medium.

**Instrumentation.** Electrophoretic mobility ( $\zeta$ -potential) measurements were made using a Malvern ZetaSizer NanoZS operating in the fast field reversal mode (phase analysis light scattering, PALS) equipped with an MPT-2 automatic titrator.

**Data Analysis.** The directly measured quantities were the pH, the conductivity ( $\mu\text{S/cm}$ ), the base 10 logarithm of the conductivity, ( $\mu\text{S/cm}$ ), and the electrophoretic mobility. EXCEL files were prepared for all three variables in a format suitable for data analysis using proprietary software algorithms, SURFER,<sup>27</sup> and two types of analyses were carried out as described previously.<sup>18</sup> The logarithmic scale for the conductivity is consistent with the free energy driving force, which is logarithmic in concentration. The choice of  $\mu\text{S/cm}$  for the units of conductivity places a scale zero near the conductivity of ambient-CO<sub>2</sub>-equilibrated distilled water and gives small whole numbers which increase with the concentration of salt.

The electrophoretic mobility is used in the representation of all EF contour and wireframe maps, because it is independent of any theoretical model for the double layer. Otherwise, reported  $\zeta$ -potential results are based on values obtained from the Smoluchowski approximation (the  $\zeta$ -potential is directly proportional to the mobility), assumed to be applicable here.

## Results and Discussion

**Validating the Data Quality of the PALS Measurement of Electrophoretic Mobility.** The electrophoretic mobility is measured by applying an electric field that causes particles (or biological cells) to migrate in proportion to their surface charge and by tracking the motion using light scattering. In practice the field is alternated, at around 20 Hz, to prevent polarization at the electrodes. Movement of the sample material, i.e., biological cells, particles, etc., in the electric field manifests itself as a

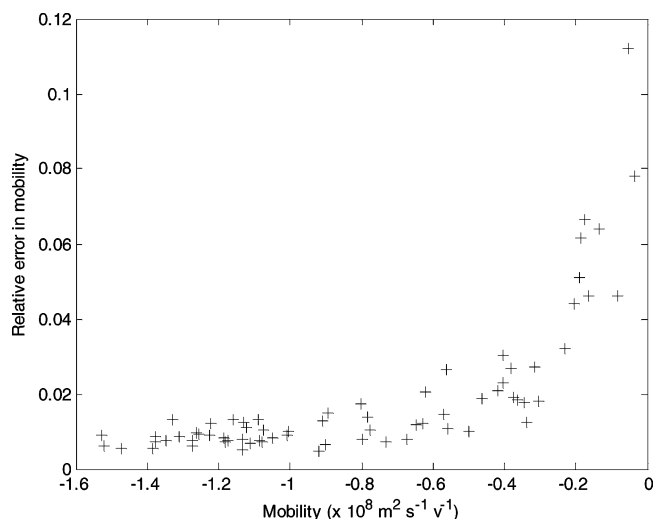


**Figure 2.** Relative error in mobility against mobility.

Doppler frequency shift in the scattered light, and in the PALS method, this frequency shift is determined by a process known as phase quadrature, which is able to measure very small frequency shifts.<sup>28,29</sup>

In ELS (electrophoretic light scattering) the solution conductance is first measured to establish the electric field, the value of which directly affects the particle velocity. Should the cell electrodes be damaged or coated or become polarized, the measured conductance will vary, so the electric field will not be well-defined. Therefore, the measured conductance is monitored for each data point and is used in the present work so that outliers are removed.

There are also other factors that affect the reproducibility and repeatability of the measured electrophoretic mobility value. Given the complex surface chemical nature of biological cells, generally all data points are included in the EF analysis. Nevertheless, criteria were established for evaluating the raw measurement data from the ZetaSizer NanoZS; this was decided since future work will involve virions and recombinant gp120/140 proteins (in the HIV envelope) from different isolates. Although this is not an issue with the current cells under study, in future studies it is expected that the sample quantity will be limited, thus severely reducing the total number of data points available for analysis.

The electric field used in the ZetaSizer NanoZS is a switched square wave that gives rise to a linear phase shift. We can therefore associate the success of the measurement of the mobility by the degree of linear dependence of the phase shift with time during each field cycle. This procedure has been carried out on each of the data sets; both the linear correlation coefficient and the error in the slope have been derived from the covariance matrix of the linear fit. These two quantities are graphed (Figure 1) for a representative data set of 60 measurements (Molt4 cells in 0.2 M sodium chloride). The correlation coefficient and the relative error in the mobility generally track each other as expected; the lowest value of correlation (0.6) and the highest relative error (0.11) correspond to the second lowest absolute mobility value recorded ( $-0.04$ ). In the measurement of electrophoretic mobility a relative error of 0.05 is expected in "typical" measurements,

(28) Miller, J. F.; Schatzel, K.; Vincent, B. *J. Colloid Interface Sci.* **1991**, *143*, 532.

(29) Tscharnuter, W. W.; McNeil-Watson, F.; Fairhurst, D. In *Particle Size Distribution III: Assessment and Characterization*; Provder, T., Ed.; ACS Symposium Series 693; American Chemical Society: Washington, DC, 1998; Chapter 22.

(26) Lusso, P.; Cocchi, F.; Balotta, C.; Markham, P. D.; Louie, A.; Farci, P.; Pal, R.; Gallo, R. C.; Reitz, M. S., Jr. *J. Virol.* **1995**, *69*, 3712.

(27) Golden Software, Inc., 809 14th St., Golden, CO 80401.



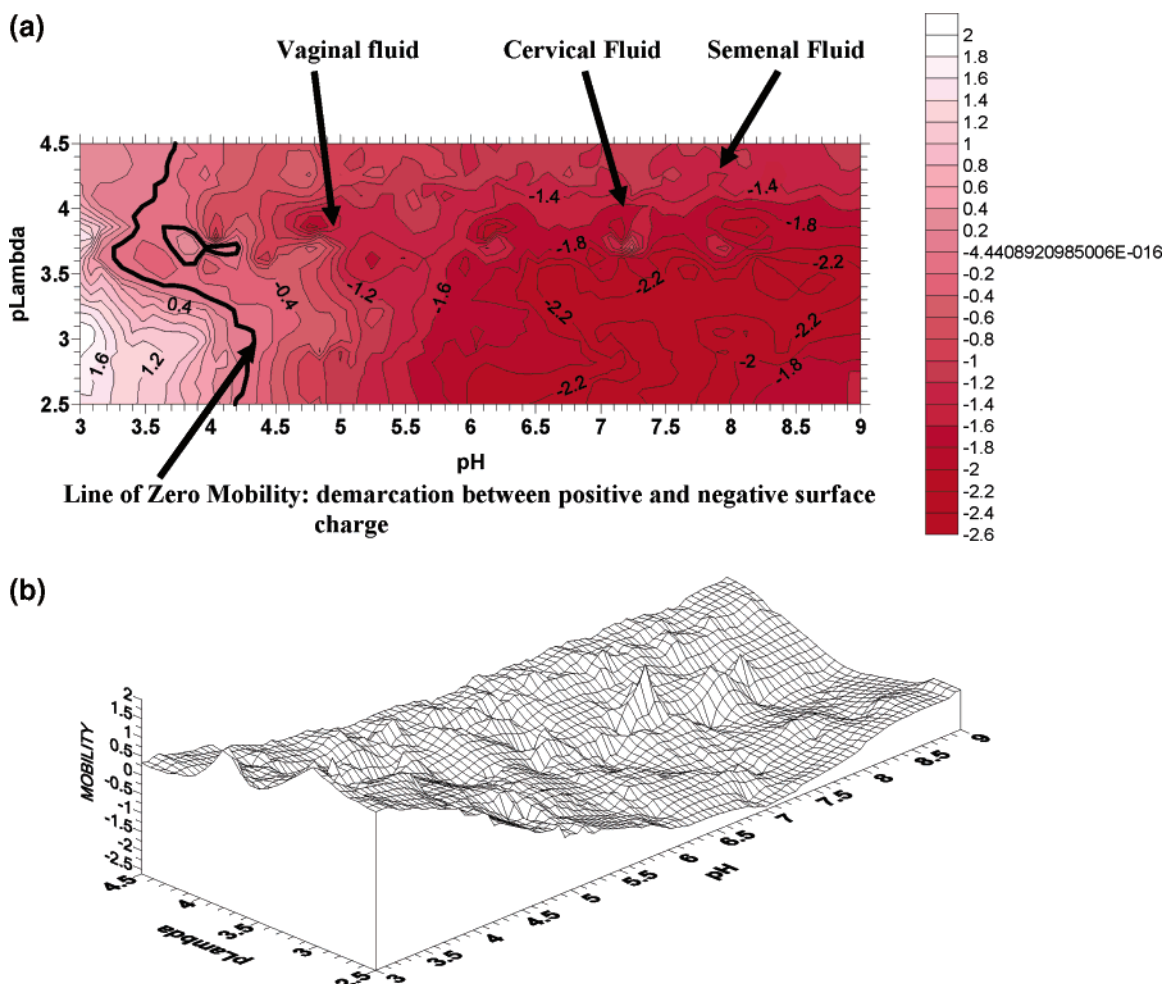


**Figure 3.** (a) EF contour map of H9 cells. (b) EF wireframe map of H9 cells corresponding to (a).

so we have confidence that the low-mobility areas of the plots have been located with sufficient accuracy.

The mobility data (Figure 2) show that the fit error is less than about 0.05 for absolute mobility values higher than about 0.2. We conclude then that any trends seen in the electrophoretic mobility as a function of pH, or other parameters (such as  $p\lambda$ ), are to be valid. The use of repeat measurements of individual points and complete data sets also gives a high value of confidence in the results.

**Electrophoretic Fingerprint of H9 Cells.**<sup>18</sup> The CD4+ H9 cell system has previously been explored in some detail over the pH range from 3.0 to 9.0 and at conductivity,  $p\lambda$ , from 2.5 to 4.5. The EF is represented in contour form in Figure 3a and in 3-D wireframe form in Figure 3b. The topography of the fingerprint is reproducible and statistically significant: three separate cultures prepared at different times; in all, a total of 982 data points were used.

A color scale has been added in Figure 3a: red for negative mobilities that tones to pink at zero mobility and then bleaches to white (blank) at maximum positive mobility. The line of zero mobility (LZM) is in bold to emphasize the demarcation between positive and negative surface charge; all of the mobility values to the left of the LZM are positive.

There are four principal features<sup>18</sup> of the H9 EF that suggest the nature of the surface chemistry of the system.

(1) Alkaline maximum. The negatively charged alkaline maximum has a narrow dome around  $p\lambda$  3.3, extending over a range in pH from 7.3 to 8.5. This seems to be characteristic of a surface carboxyl group.

(2) Acid maximum. The positively charged acid maximum around pH 3.1,  $p\lambda$  2.7, probably arises from the protonation of a group with properties of a Lewis base (discussed in more detail below).

(3) LZM. The LZM traces an S-shaped curve in the region from pH 3 to pH 4; it follows a canyon wall as opposed to a valley in pH– $p\lambda$  space since the mobility develops a sharp positive maximum at lower pH and a broad negative maximum at higher pH. The position, and meandering, of the LZM in pH– $p\lambda$  space is similar to that previously observed in amidine–carboxyl zwitterionic systems.<sup>30,31</sup>

(4) LZM loop in the pH 3.8,  $p\lambda$  3.7 region. This feature could have arisen from the statistical analysis of the SURFER program and might be regarded as an artifact since the data are limited in that region. A more plausible interpretation is that the LZM opens up into a plateau of zero mobility so that the colloid is neutral in charge over a small region in pH– $p\lambda$  space. LZM loops arise when the surface charge is near zero over a significant region in pH– $p\lambda$  space, and they encircle a center of the opposite

(30) Rowell, R. L.; Shiao, S. J.; Marlow, B. J. In *Particle Size Distribution II*; Provder, T., Ed.; ACS Symposium Series 472; American Chemical Society: Washington, DC, 1991; Chapter 21, p 326.

(31) Rowell, R. L.; Yezek, L. P.; Bishop, R. J. In *Particle Sizing and Characterization*; Provder, T., Texter, J., Eds.; ACS Symposium Series 881; American Chemical Society: Washington, DC, 2004; p 201. Yezek, L.; Rowell, R. L. *Langmuir* **2000**, *16*, 5365.

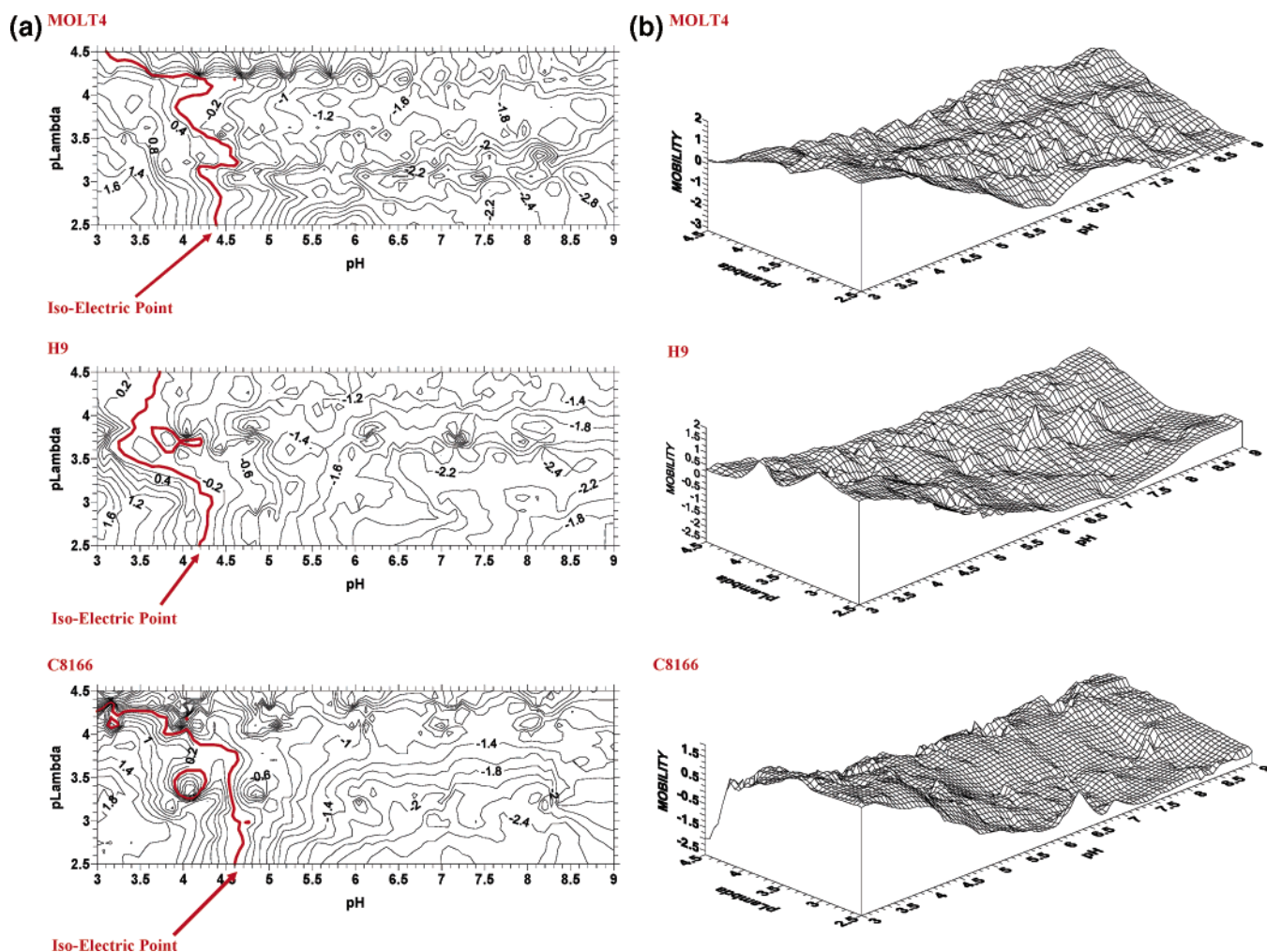


**Figure 4.** (a) Comparison of the EF contour maps for the three cell lines Molt4, H9, and C8166. (b) Comparison of the EF wireframe maps for Molt4, H9, and C8166.

charge; this may be an artifact, or it may be a real fluctuation in the measurements.

**Comparison of the EFs for the Three CD4<sup>+</sup> Cell Lines Molt4, H9, and C8166.** The EFs for both Molt4 and C8166 are constructed from cultures run in triplicate; the total number of data points used was 1194 and 1423, respectively. The contour plots and wireframes (each scaled to the same pH–p $\lambda$  ranges) are shown in parts a and b, respectively, of Figure 4. The Molt4 and C8166 systems are similar to H9 in that they present a “twisted ribbon” contour in pH–p $\lambda$  space with spherical-like domes at low and high pH arising from the pH-driven ionization of amino and carboxyl groups. Thus, a distinguishing feature of the surface chemistry of all three cell lines is the zwitterionic nature of the surface charge. However, the systems show sufficiently different characteristics that can be identified by the following properties.

(1) Difference in the path traced by the LZM. Thus, positively charged (cationic) and negatively charged (anionic) probe molecules representing real, or simulated, microbicide actives would be expected to dramatically change the pattern of the electrophoretic fingerprint since electrostatic forces would be expected to be dominant over a wide range in pH and p $\lambda$ .

(2) Extent of the positive and negative regions of maximum mobility. They differ significantly in both magnitude and extent. The properties are clearly shown despite the dynamics of growing samples, different sample batches, and samples taken at different stages during growth. The patterns are extremely sensitive to

surface charge and would be expected to change dramatically with interactions with microbicide actives or other probe molecules.

(3) Magnitude of the positive and negative charges and the ratio of the magnitudes for each species.

(4) Different isoelectric points (IEPs). The classic isoelectric point is found using a plot of  $\zeta$ -potential as a function of pH and is, ideally, a point on the pH axis where curves at different salt concentrations have a common intersection at zero  $\zeta$ -potential. In our work, we prefer to use the directly measured quantity, the electrophoretic mobility, because it is independent of any theoretical model of the double layer. In the Smoluchowski approximation, assumed to be applicable here, the  $\zeta$ -potential is directly proportional to the mobility. The IEP may be estimated as the intersection of the LZM with the envelope of accessible measurements,<sup>30</sup> here the p $\lambda$  2.5 axis.

**Nature of the Cell Surface Charge.** Simplistically, the surfaces of all three cells are comprised of proteins, carbohydrates, and lipids; the contribution of each to the surface charge is not known. We assume here that the surface charge arises primarily from ionization of protein functional groups. The building blocks of the proteins are the common  $\alpha$ -amino acids so that the charge may be expected to arise from the following groups: (1) negative charge from terminal  $\alpha$ -amino acids (probably a small contribution), (2) negative charge from the terminal carboxyl group of the side chain of aspartate, (3) negative charge from the terminal carboxyl group of the side chain of glutamate, (4) positive charge

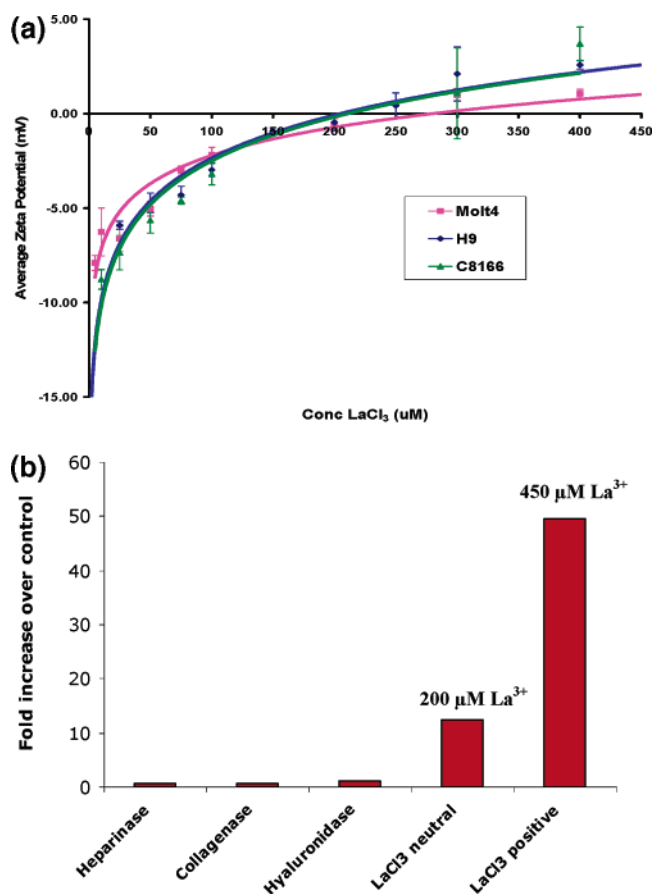
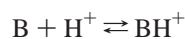


**Figure 5.** (a) Titration of CD4<sup>+</sup> T-cells with lanthanum chloride. (b) Effect of La<sup>3+</sup> cation adsorption on HIV infection.

from the terminal amino group of the side chain of lysine, (5) positive charge from the terminal amidine group of the side chain of arginine, (6) positive charge from the terminal imidazole group of the side chain of histidine. Groups 2 and 3 are acids, and charge formation is by dissociation according to the general form



Groups 4–6 are bases, and charge formation is by association according to the general form



Thus, there are at least five different characteristic equilibrium constants for the different functional groups that contribute to the total particle charge depending on the solution pH and the surface concentration of each group.

Free terminal  $\alpha$ -amino acid groups are expected to play a minor role but will have both an acid and a basic equilibrium where the carboxyl group is fully ionized at high pH while the amino group assumes maximum protonation at very low pH. The ionization of carboxyl and amino groups is well established. It is also known that the imidazole group of histidine can bind or release protons near physiological pH.<sup>32</sup> The membranes of T-cells contain glycoproteins—in particular a preponderance of *N*-acetylgalactosamine and *N*-acetylglucosamine, both of which contain an amide link that is another site for proton attachment.<sup>33</sup>

(32) Berg, J. M.; Tymoczko, J. L.; Stryer, L. *Biochemistry*, 5th ed.; W. H. Freeman: New York, 2002.

(33) Anderson, R. E.; Standefer, J. C.; Scaletti, J. V. *Lab. Invest.* **1977**, *37*, 329.

It is clear from the foregoing that the detailed surface chemistry of cells is very complex. The EF approach nevertheless allows us to probe this nondestructively.

**Comparison with EF Results from Studies of Model Colloids (Nonbiologic).** In earlier work,<sup>30</sup> the EF of a carboxyl–amidine zwitterionic polymer latex (Interfacial Dynamics Corp. (IDC) no. 2-73-70) revealed an LZM that began at pH 4.0, pI 1.6 (the lowest accessible pI) and was independent of pH up to about pI 4.0, and then it appeared to drift to lower pH (although the data in that region were obtained by extrapolation).

Later,<sup>31</sup> the EF for a different carboxyl–amidine zwitterionic polymer latex, (IDC no. 10-62-40) was determined in four supporting electrolytes: KCl, NaCl, KNO<sub>3</sub>, and NaNO<sub>3</sub>. In KCl, the LZM had an origin at pH 2.5, pI 3.0, and it drifted slightly to pH 2.9, pI 3.7. In NaCl, the LZM had an origin at pH 3.1, pI 2.2, and it curved slightly to the acid side to pH 2.8, pI 3.72. In KNO<sub>3</sub>, the LZM had an origin at pH 3.2, pI 1.9 and moved nearly independent of pH up to pI 3.9. Finally, in NaNO<sub>3</sub>, the LZM had an origin at pH 3.0, pI 2.3 and moved up, curving slightly, to pH 3.3, pI 3.9. The overall patterns were similar, but clearly there were small specific salt effects; the most different was the KCl system.

More recently,<sup>34</sup> the IEPs for 12 preparations of zwitterionic latexes have been reported in a classical electrophoresis study. These IEPs can be related to the previous LZMs only by comparing the origin of the LZM with the classical IEP. Three of the IEPs can be rejected as being out of statistical significance with the other nine preparations, resulting in a mean and standard deviation of  $4.2 \pm 0.3$  for the IEP. This can be compared with a value of pH 4.0 for the work reported in ref 30 and values of pH 2.5, 3.1, 3.2, and 3.0 for the work in ref 31. The initiators for the IDC latexes were unknown since they were commercially manufactured materials, but the polymer latex preparation for the work of ref 34 used azobis[cyanopentanoic acid] and azobis[isobutyramidine] dihydrochloride; both of these initiators are more likely to produce short side chains similar to those occurring in the cell lines studied in the present work. We note that our LZMs for Molt 4, C8166, and H9, at a pI of 2.5, originate at pH values of 4.4, 4.6, and 4.2, respectively, thus supporting our contention that all three cell lines are zwitterionic. Both H9 and C8166 also show LZM loops in the regions pH 3.8, pI 3.7 and pH 4.1, pI 3.4, respectively.

**Interpretation of EF.** EF, by itself, is a nondestructive approach to mapping the behavior of a charged particulate system as a function of the bulk pH and bulk pI. The bulk pH may differ from the local pH in the vicinity of a particle, which may in turn differ from the surface pH of the particle; however, it is an important thermodynamic variable that has proven to be useful in the characterization of charged colloids. The bulk pI is characteristic of the active electrical state in a thermodynamic sense and is a measure of contributions from the charged particles as well as the electrolyte in the medium. It should be distinguished from the ionic strength in that it measures contributions from the colloid, the salt concentration, and the changes in conductivity due to changes in pH that are frequently ignored in calculating the ionic strength.

It would be desirable to have the companion analysis, hydrodynamic fingerprinting (HF), a contour map of hydrodynamic size as a function of pH and pI, plus EF and HF contour maps as a function of mass concentration. The limited availability of sufficient sample and a precaution of preserving the viability of the samples, to allow meaningful application to real systems, limited the analysis to EF alone. It should also be mentioned that

(34) Bolt, P. S.; Goodwin, J. W.; Ottewill, R. H. *Langmuir* **2005**, *21*, 9911.



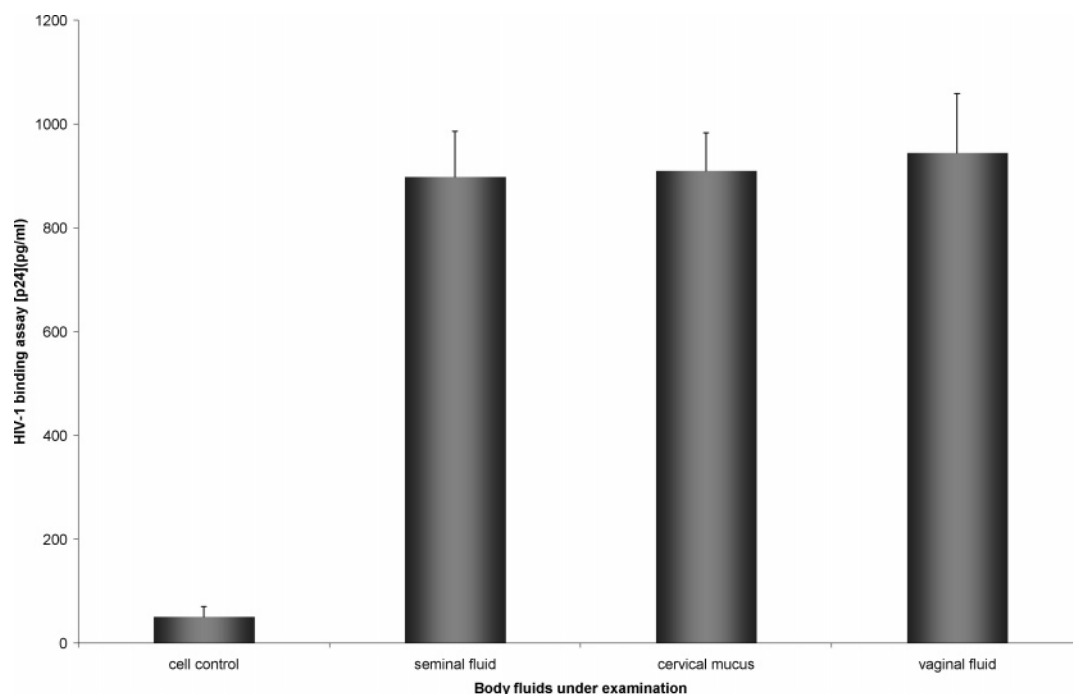


**Figure 6.** Effect of physiological fluids on HIV-1 binding to T-cells.

the methodology is also noninvasive only to the extent that the pH and electrolyte concentration do not significantly alter the local microstate properties of the charged particles. All of these considerations must be kept in mind in the interpretation of the data.

In the absence of a theory encompassing both EF and HF, it is helpful to draw attention to the work of Schulz, Gisler, Borkovec, and Sticher,<sup>35</sup> who have considered the charge on functionalized latex spheres including those with a carboxyl surface and a zwitterionic surface.

### Preliminary Biological Infectivity Measurements

**Adsorption of the  $\text{La}^{3+}$  Cation onto CD4+ Cells and Its Effect on Surface Charge and HIV Infectivity.** A study of murine sarcoma virus (MSV) showed that pretreatment with simple cations, such as  $\text{Ca}^{2+}$  and  $\text{Mg}^{2+}$ , increases infectivity and suggests that they can also affect HIV replication.<sup>36</sup> Assuming that the MSV virion carries net negative charge, then adsorption of these cations will tend to render the surface charge positive, or at least neutral. This being so, on the basis of pure colloid science principles (Schulze–Hardy),  $\text{La}^{3+}$  should have an even higher attraction affinity to a negatively charged cell surface and, therefore, could be a potential blocking agent for viral replication. Accordingly, lanthanum chloride,  $\text{LaCl}_3$ , was chosen as the test probe (it is very water soluble and, at the concentrations used, is known to be nontoxic to cells). The results for the adsorption of  $\text{La}^{3+}$  onto the three cell lines are shown in Figure 5a. In each case, there is an initial rapid increase in  $\zeta$ -potential followed by a much slower increase; there were no major fluctuations in charge, and the data were reproducible. The adsorption isotherms for the H9 and C8166 cells were virtually identical: about  $200 \mu\text{M}$   $\text{La}^{3+}$  was necessary to reduce the cell's  $\zeta$ -potential to near zero. The adsorption isotherm for Molt4 cells differed slightly; the effect of  $\text{La}^{3+}$  was less pronounced, and  $300 \mu\text{M}$   $\text{La}^{3+}$  was needed to achieve zero  $\zeta$ -potential. It is not

known if this difference is biologically significant, but unlike the H9 and C8166 cells, the Molt4 cells grow as single cells in suspension.

In the MSV study, the concentration of  $\text{Ca}^{2+}$  used to promote MSV infectivity was 20 mM. The concentration range of  $\text{La}^{3+}$  needed to render the CD4+ cell's  $\zeta$ -potential positive was found to be much lower, ca. 0.2–0.45 mM, and this is entirely in accord with the Schulze–Hardy prediction. Interestingly, the overall ZP/[ $\text{La}^{3+}$ ] profiles are very similar to that found for the flocculation of heterogeneous surfaces such as paper pulp and wastewater using polyvalent cations such as  $\text{Al}^{3+}$  and  $\text{Fe}^{3+}$ .<sup>37,38</sup>

The results clearly demonstrate that the charge characteristics of CD4+ cells can be changed by addition of small polyvalent cations.

On the basis of the above results, two solution conditions were then chosen for a replication experiment using H9 cells: (i) a just neutralized cell surface (using about  $200 \mu\text{M}$   $\text{La}^{3+}$ ) and (ii) a slightly positive cell surface (using about  $450 \mu\text{M}$   $\text{La}^{3+}$ ). The results are shown in Figure 5b.

Previous experiments (SGUL unpublished) had demonstrated that pretreatment of H9 cells with different enzymes (heparinase, collagenase, and hyaluronidase) had no overall effect on the net negative surface charge. Not unexpectedly, the current data obtained show little detectable RT activity (an indicator of viral replication) in the H9 enzyme-treated preparations. However, cells that were pretreated with  $\text{LaCl}_3$  to make them neutrally or positively charged quite clearly showed increased levels of HIV-1 replication compared to the uninfected cell control. Indeed, the positively charged cells showed a 50-fold increase in viral activity, indicating therefore that modulation of the negative surface charge on the T-cell surface profoundly affects the infection kinetics. Further work in this area using the other cell lines (Molt4 and C8166) is ongoing.

**Effect of Physiological Conditions on HIV-1 Binding to H9 Cells.** The surface characteristics that would exist under the pH/pI conditions of physiological fluids (cervical mucous, plasma

(35) Schulz, S. F.; Gisler, T.; Borkovec, M.; Sticher, H. *J. Colloid Interface Sci.* **1994**, *164*, 88.

(36) Hesse, J.; Ebbesen, P.; Kristensen, G. *Intervirology* **1978**, *9*, 173.

(37) Riddick, T. M. *Tappi* **1964**, *47*, 171.

(38) Williams, R. L. *J. Am. Water Works Assoc.* **1965**, *57*, 801.



exudates, and semen at a salt concentration comparable to 154 mM NaCl and various pH values) can readily be determined from inspection of Figure 3a. However, it is clear that the surface chemistry *in vivo* could be radically different bearing in mind that such fluids also contain species other than simple ions, e.g., proteins, that will adsorb onto the cell surface, thus altering the chemical characteristics. This aspect is currently under investigation.

The effects of these different environments on viral binding were assessed and are summarized in Figure 6. These data suggest that HIV interaction with target cells is enhanced by physiological fluids. This result is not surprising in light of the  $\text{La}^{3+}$  adsorption experiment above since it is known that physiological fluids contain various polycation species.<sup>23,24</sup> It suggests that chelating agents may be of use in microbicides to neutralize the effects of any polycations that may be present in fluids in the female lower reproductive tract.

### Relevance to HIV Infection

First, we reiterate that this is a work in progress and that the current data have, not unexpectedly, raised a number of points that bear further investigation. Work is in progress to digest off all surface protein (using a cocktail of enzymes) to expose only lipids; this will determine the contribution of protein vs lipid to the surface charge. We have also recently completed EF measurements using a series of both activated cells and primary cells; the results of this study will be the subject of a third paper. We also need to point out that the current data are obtained using *model* cells and may not fully represent *in vivo* realities and could, therefore, lead to misleading conclusions. Further, we do not know the effect of variations in the growth media on the surface charge. How does pretreatment of cells with seminal plasma change their  $\zeta$ -potential, etc.?

The ultimate goal is to study HIV and its interactions with potential microbicide actives. Work on the model (T-cell) systems will provide a better understanding of the effects of solution pH and conductivity that can be extended to HIV. This is crucial since the actual conductivity in the vaginal tract can vary enormously depending on the health of the epithelial tissue, cycle status, use of vaginal preparations, intercourse, etc. Also, importantly, although each of the T-cell lines is zwitterionic, there are real differences in the extent and distribution of the surface (carboxyl and amino) moieties, suggesting serious implications as to the charge characteristics of whole virions that partially derive their surface from host cells. Harvesting from

different cell types, different viral phenotypes, different immune cell populations, etc. will all likely have an impact on the viral surface chemistry and thus on any experiments in which they are used.

The measurements provide data purely from a simple physicochemical perspective, and our analysis and interpretation reflects this. However, the overall research must bear in mind the practical ends of the problem. For example, it is known that the pH of a healthy vagina is in the range of 4–6 and that the pH of semen is in the range of 6–8. The current study seems to suggest that the CD4+ T-cell surface, which is permissive for HIV-1 replication, is zwitterionic. In general, the surface is maximally negatively charged in alkaline conditions as might be experienced in the presence of semen. The surface is positively charged under acidic conditions similar to those encountered in the vagina. The actual degree of surface charge is also dependent upon the prevailing conductivity of the vaginal fluids. These results suggest that the best candidate for a microbicide active needs to be zwitterionic to be able to mirror the shift in sign of surface charge as the pH of the vaginal tract changes. In addition, the formulation of any topical microbicide might need to include a swamping concentration of electrolyte to provide conductivity in excess of that found in vaginal fluids to eliminate any potential shifts in IEP. It might also be appropriate to include a chelating agent to neutralize the effects of any polyvalent cations found in physiological fluids. There are meaningful practical difficulties in reducing these theoretical approaches to practice. Still, an understanding of them can only help in the development of an effective microbicide.

### Conclusion

This study has generated speculative, yet important, data concerning the relation of cell surface charge and HIV infectivity. These data provide core information on the physicochemical properties of model cellular targets for HIV-1 infection and pave the way for rational development of charge-based intervention strategies designed to prevent sexual transmission of HIV-1 infection. The results suggest that the chemical composition (formulation) of a topical microbicide can directly impact polyanion performance and the response of HIV-1 and target cells.

Work is currently in progress to determine the EF (i) for various recombinant gp120/140 proteins from different isolates and (ii) for CD4, CCR5, and CXCR4.

LA063043N